



Towards the optical second verifying optical clocks at the SI limit

McGrew, W. F.; Zhang, X.; Leopardi, H.; Fasano, R. J.; Nicolodi, D.; Beloy, K.; Yao, J.; Sherman, J. A.; Schaffer, S. A.; Savory, J.; Brown, R. C.; Romisch, S.; Oates, C. W.; Parker, T. E.; Fortier, T. M.; Ludlow, A. D.

Published in:
Optica

DOI:
[10.1364/OPTICA.6.000448](https://doi.org/10.1364/OPTICA.6.000448)

Publication date:
2019

Document version
Publisher's PDF, also known as Version of record

Document license:
[CC BY](https://creativecommons.org/licenses/by/4.0/)

Citation for published version (APA):
McGrew, W. F., Zhang, X., Leopardi, H., Fasano, R. J., Nicolodi, D., Beloy, K., ... Ludlow, A. D. (2019). Towards the optical second: verifying optical clocks at the SI limit. *Optica*, 6(4), 448-454.
<https://doi.org/10.1364/OPTICA.6.000448>



Towards the optical second: verifying optical clocks at the SI limit

W. F. MCGREW,^{1,2} X. ZHANG,¹ H. LEOPARDI,^{1,2} R. J. FASANO,^{1,2} D. NICOLDI,^{1,2} K. BELOY,¹ J. YAO,^{1,2} J. A. SHERMAN,¹ S. A. SCHÄFFER,^{1,3} J. SAVORY,¹ R. C. BROWN,^{1,4} S. RÖMISCH,¹ C. W. OATES,¹ T. E. PARKER,^{1,5} T. M. FORTIER,^{1,6} AND A. D. LUDLOW^{1,2,7}

¹National Institute of Standards and Technology, 325 Broadway, Boulder, Colorado 80305, USA

²Department of Physics, University of Colorado, Boulder, Colorado 80309, USA

³Niels Bohr Institute, University of Copenhagen, Blegdamsvej 17, 2100 Copenhagen, Denmark

⁴Present address: Georgia Tech Research Institute, Atlanta, Georgia 30332, USA

⁵e-mail: tom.parker@nist.gov

⁶e-mail: tara.fortier@nist.gov

⁷e-mail: andrew.ludlow@nist.gov

Received 8 February 2019; revised 8 March 2019; accepted 11 March 2019 (Doc. ID 359640); published 11 April 2019

The pursuit of ever more precise measures of time and frequency motivates redefinition of the second in terms of an optical atomic transition. To ensure continuity with the current definition, based on the microwave hyperfine transition in ^{133}Cs , it is necessary to measure the absolute frequency of candidate optical standards relative to primary cesium references. Armed with independent measurements, a stringent test of optical clocks can be made by comparing ratios of absolute frequency measurements against optical frequency ratios measured via direct optical comparison. Here we measure the $^1\text{S}_0 \rightarrow ^3\text{P}_0$ transition of ^{171}Yb using satellite time and frequency transfer to compare the clock frequency to an international collection of national primary and secondary frequency standards. Our measurements consist of 79 runs spanning eight months, yielding the absolute frequency to be 518 295 836 590 863.71(11) Hz and corresponding to a fractional uncertainty of 2.1×10^{-16} . This absolute frequency measurement, the most accurate reported for any transition, allows us to close the Cs-Yb-Sr-Cs frequency measurement loop at an uncertainty $< 3 \times 10^{-16}$, limited for the first time by the current realization of the second in the International System of Units (SI). Doing so represents a key step towards an optical definition of the SI second, as well as future optical time scales and applications. Furthermore, these high accuracy measurements distributed over eight months are analyzed to tighten the constraints on variation of the electron-to-proton mass ratio, $\mu = m_e/m_p$. Taken together with past Yb and Sr absolute frequency measurements, we infer new bounds on the coupling coefficient to gravitational potential of $k_\mu = (-1.9 \pm 9.4) \times 10^{-7}$ and a drift with respect to time of $\frac{\dot{\mu}}{\mu} = (5.3 \pm 6.5) \times 10^{-17}/\text{yr}$. © 2019 Optical Society of America under the terms of the [OSA Open Access Publishing Agreement](#)

<https://doi.org/10.1364/OPTICA.6.000448>

1. INTRODUCTION

Since the first observation of the 9.2 GHz hyperfine transition of ^{133}Cs , it was speculated that atomic clocks could outperform any conventional frequency reference, due to their much higher oscillation frequency and the fundamental indistinguishability of atoms [1]. Indeed, Harold Lyons' 1952 prediction that "an accuracy of one part in ten billion may be achieved" has been surpassed one million-fold by atomic fountain clocks with systematic uncertainties of a few parts in 10^{16} [2]. The precision of atomic frequency measurements motivated the 1967 redefinition of the second in the International System of Units (SI), making time the first quantity to be based upon the principles of nature, rather than upon a physical artifact [3]. The superior performance of atomic clocks has found numerous applications, most

notably enabling global navigation satellite systems (GNSS), where atomic clocks ensure precise time delay measurements that can be transformed into position measurements [4].

Microwave atomic fountain clocks exhibit a quality factor on the order of 10^{10} , and the current generation can determine the line center at 10^{-6} of the linewidth. This, along with a careful accounting of all systematic biases, leads to an uncertainty of several parts in 10^{16} , i.e., the SI limit. Significant improvement of microwave standards is considered unrealistic; however, progress has been realized utilizing optical transitions, where the higher quality factor of approximately 10^{15} allows many orders of magnitude improvement [5,6]. For example, a recent demonstration of two ytterbium optical lattice clocks at the National Institute of Standards and Technology (NIST) found instability, systematic

uncertainty, and reproducibility at the 1×10^{-18} level or better, thus outperforming the current realization of the second by a factor of >100 [7]. The superior performance of optical clocks motivates current exploratory work aimed at incorporating optical frequency standards into existing time scales [8–13]. Furthermore, for the first time, the gravitational sensitivity of these clocks surpasses state-of-the-art geodetic techniques and promises to find application in the nascent field of chronometric leveling [14]. Optical frequency references could potentially be standards not only of time, but of space-time.

Towards the goal of the eventual redefinition of the SI unit of time based on an optical atomic transition, the International Committee for Weights and Measures (CIPM) in 2006 defined secondary representations of the second so that other transitions could contribute to the realization of the SI second, albeit with an uncertainty limited at or above that of cesium (Cs) standards [15]. Optical transitions designated as secondary representations (eight at the time of this writing) represent viable candidates for a future redefinition to an optical second, and the CIPM has established milestones that must be accomplished before adopting a redefinition [16]. Two key milestones are absolute frequency measurements limited by the $\approx 10^{-16}$ performance of Cs, in order to ensure continuity between the present and new definitions, and frequency ratio measurements between different optical standards, with uncertainty significantly better than 10^{-16} . These two milestones together enable a key consistency check: it should be possible to compare a frequency ratio derived from absolute frequency measurements to an optically measured ratio with an inaccuracy limited by the systematic uncertainty of state-of-the-art Cs fountain clocks. Here we present a measurement of the ^{171}Yb absolute frequency that allows a “loop closure” consistent with zero at 2.4×10^{-16} , i.e., at an uncertainty that reaches the limit given by the current realization of the SI second.

2. EXPERIMENTAL SCHEME

This work makes use of the $578 \text{ nm } ^1\text{S}_0 \rightarrow ^3\text{P}_0$ transition of neutral ^{171}Yb atoms trapped in the Lamb–Dicke regime of an optical lattice at the operational magic wavelength [17,18]. The atomic system is identical to that described in Ref. [7] and has a systematic uncertainty of 1.4×10^{-18} . We note that only two effects (blackbody radiation shift and second-order Zeeman effect) could affect the measured transition frequency at a level that is relevant for the 10^{-16} uncertainties of the present measurement. Several improvements have reduced the need to optimize experimental operation by reducing the need for human intervention. A digital acquisition system is used to monitor several experimental parameters. If any of these leaves the nominal range, data are automatically flagged to be discarded in data processing. An algorithm for automatically reacquiring the frequency lock for the lattice laser was employed. With these improvements, an average uptime of 75% per run was obtained during the course of 79 separate runs of average duration of 4.9 h, distributed over eight months (November 2017 to June 2018).

The experimental setup is displayed in Fig. 1. A quantum-dot laser at 1156 nm is frequency-doubled and used to excite the 578 nm clock transition in a spin-polarized, sideband-cooled atomic ensemble trapped in an optical lattice. Laser light resonant with the dipole-allowed $^1\text{S}_0 \rightarrow ^1\text{P}_1$ transition at 399 nm is used to destructively detect atomic population, and this signal is integrated to apply corrections of the 1156 nm laser frequency so as to stay resonant with the ultranarrow clock line. Some of this atom-stabilized 1156 nm light is sent, via a phase-noise-canceled optical fiber, to an octave-spanning, self-referenced Ti:sapphire frequency comb [19,20], where the optical frequency is divided down to $f_{\text{rep}} = 1 \text{ GHz} - \Delta$. This microwave frequency is mixed with a hydrogen maser (labeled here ST15), multiplied to a nominal 1 GHz, and the resultant $\Delta \approx 300 \text{ kHz}$ heterodyne beat note is counted.

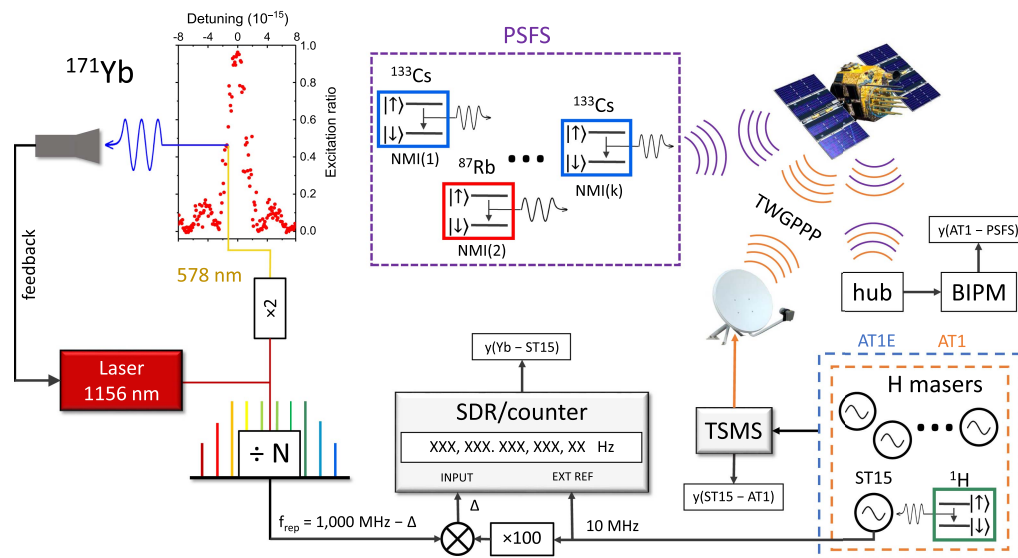


Fig. 1. Experimental setup of the Yb optical lattice standard. A counter or SDR measures the beat note between f_{rep} and the nominal 1 GHz reference derived from hydrogen maser ST15. The frequency of ST15 is compared by the NIST TSMS to that of two maser time scales—AT1E (blue) and AT1 (orange); see Supplement 1. These time scales utilize the same masers (approximately eight, including ST15) but differ in the statistical weight given to each maser [21]. The frequency of AT1 is sent to a central hub (the “star topology” used in TAI computations) via the TWGPPP protocol [22]. The measurements are then sent from the hub to the BIPM by an internet connection, and the BIPM publishes data allowing a comparison of AT1 against PSFS, composed of k separate clocks in different National Metrological Institutes (NMIs), where k varies from five to eight during the measurements.

The act of dividing the optical frequency down to 1 GHz may introduce systematic errors. Optical frequency synthesis introduces uncertainty that has been assessed through optical-optical comparisons to be well below 10^{-19} , insignificant for the present experiment [23,24]. However, for the present optical-microwave comparison, technical sources of error arising from the microwave setup may lead to inaccuracy greater by orders of magnitude. The nominal 10 MHz maser signal is multiplied by 100, to 1 GHz, by means of a frequency multiplier based on a phase-locked-loop. Electronic synthesis uncertainty is assessed by homodyne detection of the maser signal mixed with a 10 MHz signal generated by a direct digital synthesizer referenced to the 1 GHz signal. Electronic synthesis is found to contribute errors no larger than 3×10^{-17} . Another source of uncertainty arises from counting error. The first half of the data set is obtained using a 10-second-gated commercial frequency counter to count the heterodyne beat note. Counting error is assessed by measuring the 10 MHz maser signal, also used as the counter's external reference. This counting error contributes an uncertainty of as much as 6×10^{-14} of Δ , leading to an error of $<2 \times 10^{-17}$ on f_{rep} , and thus also on the optical frequency. The second half of the data set is obtained by replacing the counter with a software-defined radio (SDR) in two-channel differential mode [25]. The SDR phase continuously measured the frequency once per second with zero dead time. The hardware acquisition rate and effective (software digital filter) noise bandwidth were 1 MHz and 50 Hz, respectively. For all run durations the counting error of the SDR is $<1 \times 10^{-17}$ of f_{rep} .

After the optical signal is downconverted and compared to the hydrogen maser ST15, the comb equation is used to determine a normalized frequency difference between the Yb optical standard and the maser, $y(\text{Yb-ST15})$. Throughout this work, we express normalized frequency differences between frequency standards A and B as follows:

$$y(A - B) \equiv y_A(t) - y_B(t) = \frac{\nu_A^{\text{act}}}{\nu_A^{\text{nom}}} - \frac{\nu_B^{\text{act}}}{\nu_B^{\text{nom}}} \approx \frac{\nu_A^{\text{act}}/\nu_B^{\text{act}}}{\nu_A^{\text{nom}}/\nu_B^{\text{nom}}} - 1, \quad (1)$$

where $\nu_X^{\text{act(nom)}}$ is the actual (nominal) frequency of standard X, and the approximation is valid in the limit $(\nu_X^{\text{act}} - \nu_X^{\text{nom}})/\nu_X^{\text{nom}} \ll 1$, a well-founded assumption throughout this work. In the definition of $y(\text{Yb-ST15})$, $\nu_{\text{Yb}}^{\text{nom}} = \nu_{\text{Yb}}^{\text{CIPM17}} = 518\,295\,836\,590\,863.6$ Hz is the 2017 CIPM recommended frequency of the Yb clock transition [16] and $\nu_{\text{ST15}}^{\text{nom}} = 10$ MHz. The NIST time scale measurement system (TSMS) is used to transfer the frequency difference, $y(\text{Yb-ST15})$, from maser ST15 to a local maser time scale, labeled AT1E, which is significantly stabler than ST15. The time scale serves as a flywheel oscillator for a comparison to an average of primary and secondary frequency standards (PSFS), which the International Bureau of Weights and Measures (BIPM) publishes with a resolution of one month in Circular T [26]. The dead time uncertainty [27] associated with intermittent operation of the optical standard is comprehensively evaluated in Part A of Supplement 1 and amounts to the largest source of statistical uncertainty; see Table 1. The maser time scale frequency is transmitted to the BIPM via the hybrid Two-Way Satellite Time and Frequency Transfer/GPS Precise Point Positioning (TWGPPP) frequency transfer protocol [22], and the frequency transfer uncertainty is the second largest source of statistical uncertainty. The transfer process from the local maser time scale to PSFS is described in

Table 1. Uncertainty Budget of the Eight-Month Campaign for the Absolute Frequency Measurement of the ^{171}Yb Clock Transition

Uncertainty (10^{-16})	March 2018 ^a	Full Campaign
Type A uncertainty		
Dead time	2.5	1.0
Frequency transfer	2.6	0.9
Yb-maser comparison	0.8	0.4
Time scale measurement	<0.1	<0.1
PSFS	1.4	0.5
Total type A	4.0	1.6
Frequency comb type B uncertainty		
Optical synthesis	<0.001	<0.001
Electronic synthesis	0.3	0.3
Counter/SDR	0.1	0.1
Total comb type B	0.3	0.3
PSFS type B	1.4	1.3
Yb type B	0.014	0.014
Relativistic redshift	0.06	0.06
Total	4.2	2.1

^aData for March 2018 are shown as an example of one month's data.

Part B of Supplement 1. The frequency transfer processes from ST15 to the local maser time scale and finally to PSFS are continuously operating, thus transferring the frequencies between the standards with no dead time. However, the comparison data are published by the BIPM on a grid roughly corresponding to a month (with duration of 25, 30, or 35 days).

3. RESULTS AND ANALYSIS

We made 79 measurements over the course of eight months, for a total measurement interval of 12.1 days, or a 4.9% effective duty cycle. The weighted mean of the eight monthly values, $y_m(\text{Yb-PSFS})$, gives a value for the total normalized frequency difference obtained from these measurements, $y_T(\text{Yb-PSFS})$ and its associated uncertainty. The statistical (type A) and systematic (type B) uncertainties are accounted for in Table 1. Type B uncertainties tend to be highly correlated over time and therefore do not average down with further measurement time. For the uncertainty budgets of state-of-the-art Cs fountain clocks, the leading term is locally determined (e.g., microwave-related effects or density effects). Following convention, here we treat the type B uncertainties of the PSFS ensemble's constituent fountain clocks [28–33] as uncorrelated between standards, leading to a PSFS type B uncertainty of 1.3×10^{-16} , lower than the uncertainty of any individual fountain. We measure a value of $\nu_{\text{Yb}} = 518295836590863.71(11)$ Hz. The difference between our measurement and the CIPM recommended value is $(2.1 \pm 2.1) \times 10^{-16}$, where the stated error bar corresponds to the 1σ uncertainty of the mean value. This should be compared to the CIPM's recommended uncertainty estimation of 5×10^{-16} [16]. The reduced chi-squared statistic, χ_{red}^2 , is 0.98, indicating that the scatter in the eight monthly values is consistent with the stated uncertainties. This represents the most accurate absolute frequency measurement yet performed on any transition. Furthermore, good agreement is found between this measurement and previous absolute frequency measurements of the Yb transition (Fig. 2). If a line is fit to our data, the slope is found

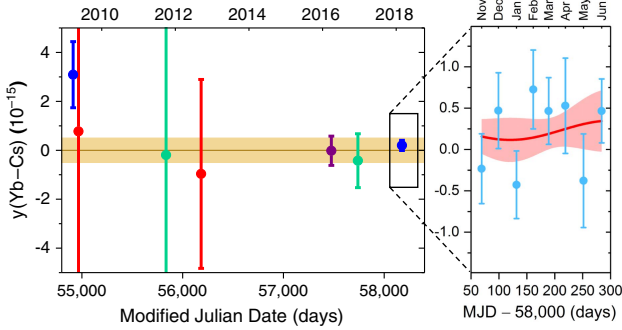


Fig. 2. Absolute frequency measurements of the $^1S_0 \rightarrow ^3P_0$ transition frequency measured by four different laboratories: NIST (blue) [18], National Metrological Institute of Japan (red) [34,35], the Korea Research Institute of Standards and Science (green) [36,37], and the Istituto Nazionale di Ricerca Metrologica (purple) [38]. The light-blue points in the inset represent the eight monthly values reported in this work, $y_m(\text{Yb-PSFS})$, and the final dark blue point represents $y_T(\text{Yb-PSFS})$. The yellow shaded region represents the 2017 CIPM recommended frequency and uncertainty. The inset shows a sinusoidal fit of the coupling parameter to gravitational potential for measurements of the frequency ratio between Yb and Cs between November 2017 and June 2018. The red shaded region in the inset represents 1σ uncertainty in the fit function.

to be $(2.0 \pm 2.2) \times 10^{-18}/\text{day}$, indicating that there is no statistically significant frequency drift.

Due to the unavailability of a local Cs primary frequency reference during this period, these measurements were performed without one. This mode of operation limits the achievable instability—with a local Cs fountain clock and a low-instability microwave oscillator, it is possible to achieve type A uncertainties at the low 10^{-16} level after one day of averaging, whereas in our configuration this was not achieved until >10 days of cumulative run time. Furthermore, it is necessary to correctly account for dead time uncertainty, as frequency measurements of the maser time scale against PSFS are published on a very coarse grid. On the other hand, the unprecedented accuracy reported in this work is directly facilitated by the lower type B uncertainty associated with the PSFS ensemble, as compared with any single Cs

fountain. An additional advantage to this mode of operation is that it is straightforward to determine frequency ratios with other secondary representations of the second that may be contributing to PSFS. For example, during these measurements, a Rb fountain clock (SYRTE FORb) contributed to PSFS [31], allowing the first direct measurement of the Yb/Rb ratio, found to be $\nu_{\text{Yb}}/\nu_{\text{Rb}} = 75\,833.197\,545\,114\,192(33)$; see Part C of Supplement 1.

It is desirable to establish the consistency of frequency ratios determined through direct comparisons and through absolute frequency measurements. For absolute frequencies, the CIPM recommended values are based upon a least-squares algorithm that takes as inputs both absolute frequency measurements, as well as optical ratio measurements [16,39]. To establish the consistency between absolute frequency measurements and direct optical ratio measurements, we determine average frequencies only from the former, as a weighted average of all previous measurements.

If $\chi_{\text{red}}^2 > 1$, we expand the uncertainty of the mean by $\sqrt{\chi_{\text{red}}^2}$. For the Yb frequency, we determine a weighted average of the present work and six previous measurements [18,34–38], $\nu_{\text{Yb}}^{\text{avg}} = 518\,295\,836\,590\,863.714(98)$ Hz, with $\chi_{\text{red}}^2 = 0.85$. For the Sr frequency, we likewise determine a weighted average of 17 previous measurements [9,10,40–54], $\nu_{\text{Sr}}^{\text{avg}} = 429\,228\,004\,229\,873.055(58)$ Hz, with $\chi_{\text{red}}^2 = 0.57$. The frequency ratio derived from absolute frequency measurements is, therefore, $\mathcal{R}_{\text{abs}}^{\text{avg}} = \nu_{\text{Yb}}^{\text{avg}}/\nu_{\text{Sr}}^{\text{avg}} = 1.207\,507\,039\,343\,337\,86(28)$. A frequency ratio can also be determined directly from optical frequency ratio measurements. From a weighted average of six optical ratio measurements [55–60], we determine $\mathcal{R}_{\text{opt}}^{\text{avg}} = 1.207\,507\,039\,343\,337\,768(60)$, with $\chi_{\text{red}}^2 = 1.28$. All three averages exhibit a χ_{red}^2 close to 1, indicating that the scatter is mostly consistent with the stated uncertainties; only the uncertainty of optical ratios is rescaled, and that only modestly. We therefore determine a loop misclosure of $(\mathcal{R}_{\text{abs}} - \mathcal{R}_{\text{opt}})/\mathcal{R} = (0.8 \pm 2.4) \times 10^{-16}$, indicating consistency between the optical and microwave scales at a level that is limited only by the uncertainties of Cs clocks. This agreement is demonstrated graphically in Fig. 3. We emphasize that each of the three legs of the loop—Yb absolute frequency, Sr absolute frequency, and

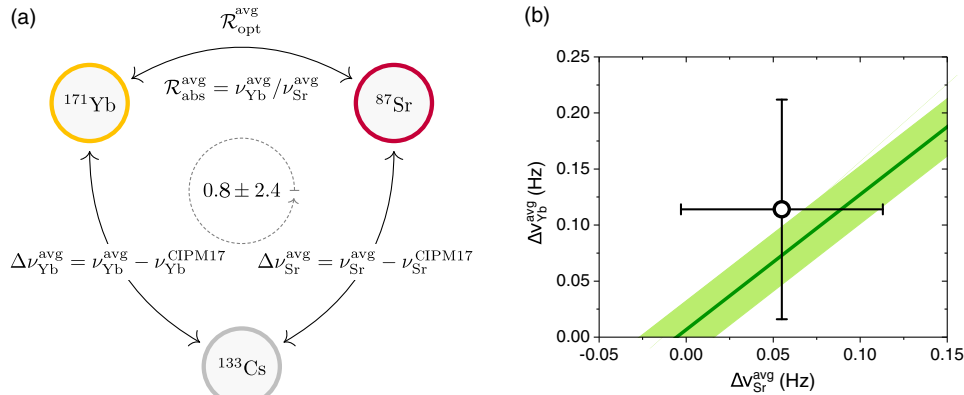


Fig. 3. Graphical representation of the agreement between frequency ratios derived from absolute frequency measurements of ^{171}Yb and ^{87}Sr and direct optical measurements. (a) Schematic of the Cs-Yb-Sr-Cs loop that is examined. The central number is the misclosure, as parts in 10^{16} . (b) Average Yb and Sr frequency, offset from the CIPM 2017 recommended values, parametrically plotted against each other. The error bars are the 1σ uncertainty in the averaged absolute frequency measurements. The optical ratio measurement (dark green) appears as a line in this parameter-space, with the shaded region representing the uncertainty of the ratio. Frequency ratios derived from absolute frequencies agree well with ratios measured optically.

Table 2. Measurements of Coupling of Dimensionless Constants to Gravitational Potential, with Sensitivity Coefficients, ΔK , from [62–64]

No.	Reference	X, Y	$\beta_{X,Y}(10^{-6})$	$\Delta K_{X,Y}^{\alpha}$	$\Delta K_{X,Y}^{X_q}$	$\Delta K_{X,Y}^{\mu}$
(i)	Dzuba & Flambaum, 2017 [65]	Al ⁺ , Hg ⁺	0.16 ± 0.30	2.95	0	0
(ii)	Ashby <i>et al.</i> , 2018 [66]	H, Cs	0.22 ± 0.25	-0.83	-0.102	0
(iii)	This work	Yb, Cs	-0.8 ± 1.4	-2.52	-0.002	-1

Yb/Sr ratio—feature different measurements performed at multiple laboratories across the world and are thus largely uncorrelated to each other.

4. NEW LIMITS ON COUPLING OF m_e/m_p TO GRAVITATIONAL POTENTIAL

Many beyond-Standard-Model theories require that parameters traditionally considered fundamental constants may vary across time and space [61]. This hypothesized variation is detectable by looking for a change in the frequency ratio of two different types of atomic clock [62]. We analyze our eight-month frequency comparison data to place bounds upon a possible coupling of the measured Yb/Cs frequency ratio to the gravitational potential of the Sun. We fit our data to $\gamma(\text{Yb-PSFS}) = A \cos(2\pi(t - t_0)/1 \text{ yr}) + y_0$, where A and y_0 are free parameters, t is the median date for each of the eight months, t_0 is the date of the 2018 perihelion, and $1 \text{ yr} = 365.26$ days is the mean length of the anomalistic year. From our data, we determine the yearly variation of the Yb/Cs ratio, $A_{\text{Yb,Cs}} = (-1.3 \pm 2.3) \times 10^{-16}$; see the inset to Fig. 2. The amplitude of the annual variation of the gravitational potential is $\Delta\Phi = (\Phi_{\text{max}} - \Phi_{\text{min}})/2 \approx (1.65 \times 10^{-10})c^2$, where c is the speed of light in vacuum. Therefore, the coupling of the Yb/Cs ratio to gravitational potential is given by $\beta_{\text{Yb,Cs}} = A_{\text{Yb,Cs}}/(\Delta\Phi/c^2) = (-0.8 \pm 1.4) \times 10^{-6}$. A nonzero β coefficient would indicate a violation of the Einstein equivalence principle, which requires that the outcome of any local experiment (e.g., a frequency ratio measurement) is independent of the location at which the experiment was performed. Here we did not observe any violation of the equivalence principle.

Were this violation to occur, it might arise due to variation of the fine structure constant, α ; the ratio of the light quark mass to the quantum chromodynamics (QCD) scale, $X_q = m_q/\Lambda_{\text{QCD}}$; or the electron-to-proton mass ratio, $\mu = m_e/m_p$. To discriminate among each of these constants, we combine our results with two previous measurements—an analysis [65] of a prior optical-optical measurement [67] and a microwave-microwave measurement [66]. These results are chosen as they exhibit sensitivities to fundamental constants that are nearly orthogonal to each other and to our optical-microwave measurement. Table 2 displays the coupling to gravitational potential observed in each measurement, as well as the differential sensitivity parameter $\Delta K_{X,Y}^{\epsilon}$, defined by $\delta y(X - Y) = \sum_{\epsilon} \Delta K_{X,Y}^{\epsilon} (\delta\epsilon/\epsilon)$, where X and Y are the two atomic clocks being compared, and ϵ is α , X_q , or μ . Values of $\Delta K_{X,Y}^{\epsilon}$ are from [62–64]. Rescaling the β parameter to sensitivity yields a parameter quantifying coupling to gravity potential, $k_{\epsilon} = \beta_{X,Y}/\Delta K_{X,Y}^{\epsilon}$. We first use line (i) of Table 2 to constrain the coupling parameter of α , $k_{\alpha} = (0.5 \pm 1.0) \times 10^{-7}$. Applying this coefficient to line (ii) and propagating the errors, we find $k_{X_q} = (-2.6 \pm 2.6) \times 10^{-6}$. Applying both of these coefficients to the present work in line (iii), we obtain a coupling coefficient to gravitational potential of $k_{\mu} = (0.7 \pm 1.4) \times 10^{-6}$. This value

represents an almost fourfold improvement over the previous constraint, $k_{\mu} = (-2.5 \pm 5.4) \times 10^{-6}$ [68]. In Part D of Supplement 1, we extend our analysis to the full record of all Yb and Sr absolute frequency measurements to infer $k_{\mu} = (-1.9 \pm 9.4) \times 10^{-7}$ and $\dot{\mu} = (5.3 \pm 6.5) \times 10^{-17}/\text{yr}$.

5. CONCLUSIONS

We have presented the most accurate spectroscopic measurement of any optical atomic transition, i.e., with the lowest uncertainty with respect to the SI realization of the second. We find that the frequency ratio derived from ¹⁷¹Yb and ⁸⁷Sr absolute frequency measurements agrees with the optically measured ratio at a level that is primarily limited by the uncertainties of state-of-the-art fountain clocks. This level of agreement bolsters the case for redefinition in terms of an optical second. Further progress can be realized by the closing of loops consisting exclusively of optical clocks, since the improved precision of these measurements will allow misclosures that are orders of magnitude below the SI limit.

Funding. National Institute of Standards and Technology (NIST); National Aeronautics and Space Administration (NASA); Defense Advanced Research Projects Agency (DARPA).

Acknowledgment. The authors thank J. C. Bergquist and N. Ashby for their careful reading of the manuscript. Initial development of the AT1 time scale was facilitated by J. Levine. We also wish to express our appreciation for the availability of data from the eight national primary and secondary fountain frequency standards reporting in Circular T; this study would have been impossible without these data.

REFERENCES

1. H. Lyons, "Spectral lines as frequency standards," *Ann. N.Y. Acad. Sci.* **55**, 831–871 (1952).
2. T. P. Heavner, E. A. Donley, F. Levi, G. Costanzo, T. E. Parker, J. H. Shirley, N. Ashby, S. Barlow, and S. R. Jefferts, "First accuracy evaluation of NIST-F2," *Metrologia* **51**, 174–182 (2014).
3. J. Terrien, "News from the International Bureau of Weights and Measures," *Metrologia* **4**, 41–45 (1968).
4. N. Ashby, "Relativity and the global positioning system," *Phys. Today* **55**(5), 41–47 (2002).
5. J. L. Hall, "Nobel lecture: defining and measuring optical frequencies," *Rev. Mod. Phys.* **78**, 1279–1295 (2006).
6. A. D. Ludlow, M. M. Boyd, J. Ye, E. Peik, and P. O. Schmidt, "Optical atomic clocks," *Rev. Mod. Phys.* **87**, 637–701 (2015).
7. W. F. McGrew, X. Zhang, R. J. Fasano, S. A. Schäffer, K. Beloy, D. Nicolodi, R. C. Brown, N. Hinkley, G. Milani, M. Schioppo, T. H. Yoon, and A. D. Ludlow, "Atomic clock performance enabling geodesy below the centimetre level," *Nature* **564**, 87–90 (2018).
8. T. Ido, H. Hachisu, F. Nakagawa, and Y. Hanado, "Rapid evaluation of time scale using an optical clock," *J. Phys. Conf. Ser.* **723**, 012041 (2016).

9. C. Grebing, A. Al-Masoudi, S. Dörscher, S. Häfner, V. Gerginov, S. Weyers, B. Lipphardt, F. Riehle, U. Sterr, and C. Lisdat, "Realization of a timescale with an accurate optical lattice clock," *Optica* **3**, 563–569 (2016).
10. J. Lodewyck, S. Bilicki, E. Bookjans, J. L. Robyr, C. Shi, G. Vallet, R. Le Targat, D. Nicolodi, Y. Le Coq, J. Guéna, M. Abgrall, P. Rosenbusch, and S. Bize, "Optical to microwave clock frequency ratios with a nearly continuous strontium optical lattice clock," *Metrologia* **53**, 1123–1130 (2016).
11. H. Hachisu, F. Nakagawa, Y. Hanado, and T. Ido, "Months-long real-time generation of a time scale based on an optical clock," *Sci. Rep.* **8**, 4243 (2018).
12. J. Yao, T. E. Parker, N. Ashby, and J. Levine, "Incorporating an optical clock into a time scale," *IEEE Trans. Ultrason. Ferroelectr. Freq. Control* **65**, 127–134 (2018).
13. J. Yao, J. Sherman, T. Fortier, H. Leopardi, T. Parker, J. Levine, J. Savory, S. Romisch, W. McGrew, X. Zhang, D. Nicolodi, R. Fasano, S. Schaeffer, K. Beloy, and A. Ludlow, "Progress on optical-clock-based time scale at NIST: simulations and preliminary real-data analysis," *Navigation* **65**, 601–608 (2018).
14. P. Delva and J. Lodewyck, "Atomic clocks: new prospects in metrology and geodesy," *Acta Futura* **7**, 67–78 (2013).
15. P. Gill and F. Riehle, "On secondary representations of the second," in *Proceedings of the 2006 Meeting of the European Frequency and Time Forum* (2006), pp. 282–288.
16. F. Riehle, P. Gill, F. Arias, and L. Robertsson, "The CIPM list of recommended frequency standard values: guidelines and procedures," *Metrologia* **55**, 188–200 (2018).
17. H. Katori, M. Takamoto, V. G. Pal'chikov, and V. D. Ovsiannikov, "Ultrastable optical clock with neutral atoms in an engineered light shift trap," *Phys. Rev. Lett.* **91**, 173005 (2003).
18. N. D. Lemke, A. D. Ludlow, Z. W. Barber, T. M. Fortier, S. A. Diddams, Y. Jiang, S. R. Jefferts, T. P. Heavner, T. E. Parker, and C. W. Oates, "Spin-1/2 optical lattice clock," *Phys. Rev. Lett.* **103**, 063001 (2009).
19. T. M. Fortier, A. Bartels, and S. A. Diddams, "Octave-spanning Ti:sapphire laser with a repetition rate >1 GHz for optical frequency measurements and comparisons," *Opt. Lett.* **31**, 1011–1013 (2006).
20. J. E. Stalnaker, S. A. Diddams, T. M. Fortier, K. Kim, L. Hollberg, J. C. Bergquist, W. M. Itano, M. J. Delany, L. Lorini, W. H. Oskay, T. P. Heavner, S. R. Jefferts, F. Levi, T. E. Parker, and J. Shirley, "Optical-to-microwave frequency comparison with fractional uncertainty of 10^{-15} ," *Appl. Phys. B* **89**, 167–176 (2007).
21. T. E. Parker, "Hydrogen maser ensemble performance and characterization of frequency standards," in *Proceedings Joint Meeting of the IEEE International Frequency Control Symposium and the European Frequency and Time Forum, Besançon, France* (1999), pp. 173–176.
22. Z. Jiang and G. Petit, "Combination of TWSTFT and GNSS for accurate UTC time transfer," *Metrologia* **46**, 305–314 (2009).
23. Y. Yao, Y. Jiang, H. Yu, Z. Bi, and L. Ma, "Optical frequency divider with division uncertainty at the 10^{-21} level," *Natl. Sci. Rev.* **3**, 463–469 (2016).
24. H. Leopardi, J. Davila-Rodriguez, F. Quinlan, J. Olson, J. A. Sherman, S. A. Diddams, and T. M. Fortier, "Single-branch Er: fiber frequency comb for precision optical metrology with 10^{-18} fractional instability," *Optica* **4**, 879–885 (2017).
25. J. A. Sherman and R. Jördens, "Oscillator metrology with software defined radio," *Rev. Sci. Instrum.* **87**, 054711 (2016).
26. <https://www.bipm.org/en/bipm/tai>.
27. D.-H. Yu, M. Weiss, and T. E. Parker, "Uncertainty of a frequency comparison with distributed dead time and measurement interval offset," *Metrologia* **44**, 91–96 (2007).
28. J. Guéna, M. Abgrall, D. Rovera, P. Laurent, B. Chupin, M. Lours, G. Santarelli, P. Rosenbusch, M. E. Tobar, R. Li, K. Gibble, A. Clairon, and S. Bize, "Progress in atomic fountains at LNE-SYRTE," *IEEE Trans. Ultrason. Ferroelectr. Freq. Control* **59**, 391–409 (2012).
29. Y. S. Dornin, V. N. Baryshev, A. I. Boyko, G. A. Elkin, A. V. Novoselov, L. N. Kopylov, and D. S. Kupalov, "The MTsR-F2 fountain-type cesium frequency standard," *Meas. Tech.* **55**, 1155–1162 (2013).
30. F. Levi, D. Calonico, C. E. Calosso, A. Godone, S. Micalizio, and G. A. Costanzo, "Accuracy evaluation of ITCsF2: a nitrogen cooled caesium fountain," *Metrologia* **51**, 270–284 (2014).
31. J. Guéna, M. Abgrall, A. Clairon, and S. Bize, "Contributing to TAI with a secondary representation of the SI second," *Metrologia* **51**, 108–120 (2014).
32. F. Fang, M. Li, P. Lin, W. Chen, N. Liu, Y. Lin, P. Wang, K. Liu, R. Suo, and T. Li, "NIM5 Cs fountain clock and its evaluation," *Metrologia* **52**, 454–468 (2015).
33. S. Weyers, V. Gerginov, M. Kazda, J. Rahm, B. Lipphardt, G. Dobrev, and K. Gibble, "Advances in the accuracy, stability, and reliability of the PTB primary fountain clocks," *Metrologia* **55**, 789–805 (2018).
34. T. Kohno, M. Yasuda, K. Hosaka, H. Inaba, Y. Nakajima, and F. L. Hong, "One-dimensional optical lattice clock with a fermionic ^{171}Yb isotope," *Appl. Phys. Express* **2**, 072501 (2009).
35. M. Yasuda, H. Inaba, T. Kohno, T. Tanabe, Y. Nakajima, and K. Hosaka, "Improved absolute frequency measurement of the ^{171}Yb optical lattice clock towards the redefinition of the second," *Appl. Phys. Express* **5**, 102401 (2012).
36. C. Y. Park, D.-H. Yu, W.-K. Lee, S. E. Park, E. B. Kim, S. K. Lee, J. W. Cho, T. H. Yoon, J. Mun, S. J. Park, T. Y. Kwon, and S.-B. Lee, "Absolute frequency measurement of $^1\text{S}_0(F=1/2)$ - $^3\text{P}_0(F=1/2)$ transition of ^{171}Yb atoms in a one-dimensional optical lattice at KRISS," *Metrologia* **50**, 119–128 (2013).
37. H. Kim, M.-S. Heo, W.-K. Lee, C. Y. Park, S.-W. Hwang, and D.-H. Yu, "Improved absolute frequency measurement of the ^{171}Yb optical lattice clock at KRISS relative to the SI second," *Jpn. J. Appl. Phys.* **56**, 050302 (2017).
38. M. Pizzocaro, P. Thoumany, B. Rauf, F. Bregolin, G. Milani, C. Clivati, G. A. Costanzo, F. Levi, and D. Calonico, "Absolute frequency measurement of the $^1\text{S}_0$ - $^3\text{P}_0$ transition of ^{171}Yb ," *Metrologia* **54**, 102–112 (2017).
39. H. S. Margolis and P. Gill, "Least-squares analysis of clock frequency comparison data to deduce optimized frequency and frequency ratio values," *Metrologia* **52**, 628–634 (2015).
40. A. D. Ludlow, M. M. Boyd, T. Zelevinsky, S. M. Foreman, S. Blatt, M. Notcutt, T. Ido, and J. Ye, "Systematic study of the ^{87}Sr clock transition in an optical lattice," *Phys. Rev. Lett.* **96**, 033003 (2006).
41. R. Le Targat, X. Baillard, M. Fouché, A. Brusch, O. Tcherbakoff, G. D. Rovera, and P. Lemonde, "Accurate optical lattice clock with ^{87}Sr atoms," *Phys. Rev. Lett.* **97**, 130801 (2006).
42. M. M. Boyd, A. D. Ludlow, S. Blatt, S. M. Foreman, T. Ido, T. Zelevinsky, and J. Ye, " ^{87}Sr lattice clock with inaccuracy below 10^{-15} ," *Phys. Rev. Lett.* **98**, 083002 (2007).
43. X. Baillard, M. Fouché, R. Le Targat, P. G. Westergaard, A. Lecallier, F. Chapellet, M. Abgrall, G. D. Rovera, P. Laurent, P. Rosenbusch, S. Bize, G. Santarelli, A. Clairon, P. Lemonde, G. Grosche, B. Lipphardt, and H. Schnatz, "An optical lattice clock with spin-polarized ^{87}Sr atoms," *Eur. Phys. J. D* **48**, 11–17 (2008).
44. G. K. Campbell, A. D. Ludlow, S. Blatt, J. W. Thomsen, M. J. Martin, M. H. G. De Miranda, T. Zelevinsky, M. M. Boyd, and J. Ye, "The absolute frequency of the ^{87}Sr optical clock transition," *Metrologia* **45**, 539–548 (2008).
45. F.-L. Hong, M. Musha, M. Takamoto, H. Inaba, S. Yanagimachi, A. Takamizawa, K. Watabe, T. Ikegami, M. Imae, Y. Fujii, M. Amemiya, K. Nakagawa, K. Ueda, and H. Katori, "Measuring the frequency of a Sr optical lattice clock using a 120 km coherent optical transfer," *Opt. Lett.* **34**, 692–694 (2009).
46. S. T. Falke, H. Schnatz, J. S. R. V. Winfred, T. H. Middelmann, S. T. Vogt, S. Weyers, B. Lipphardt, G. Grosche, F. Riehle, U. Sterr, and C. H. Lisdat, "The ^{87}Sr optical frequency standard at PTB," *Metrologia* **48**, 399–407 (2011).
47. A. Yamaguchi, N. Shiga, S. Nagano, Y. Li, H. Ishijima, H. Hachisu, M. Kumagai, and T. Ido, "Stability transfer between two clock lasers operating at different wavelengths for absolute frequency measurement of clock transition in ^{87}Sr ," *Appl. Phys. Express* **5**, 022701 (2012).
48. R. Le Targat, L. Lorini, Y. Le Coq, M. Zawada, J. Guéna, M. Abgrall, M. Gurov, P. Rosenbusch, D. G. Rovera, B. Nagórny, R. Gartman, P. G. Westergaard, M. E. Tobar, M. Lours, G. Santarelli, A. Clairon, S. Bize, P. Laurent, P. Lemonde, and J. Lodewyck, "Experimental realization of an optical second with strontium lattice clocks," *Nat. Commun.* **4**, 2109 (2013).
49. D. Akamatsu, H. Inaba, K. Hosaka, M. Yasuda, A. Onae, T. Suzuyama, M. Amemiya, and F.-L. Hong, "Spectroscopy and frequency measurement of the ^{87}Sr clock transition by laser linewidth transfer using an optical frequency comb," *Appl. Phys. Express* **7**, 012401 (2014).
50. S. Falke, N. Lemke, C. Grebing, B. Lipphardt, S. Weyers, V. Gerginov, N. Huntemann, C. Hagemann, A. Al-Masoudi, S. Häfner, S. Vogt, U. Sterr, and C. Lisdat, "A strontium lattice clock with 3×10^{-17} inaccuracy and its frequency," *New J. Phys.* **16**, 073023 (2014).

51. T. Tanabe, D. Akamatsu, T. Kobayashi, A. Takamizawa, S. Yanagimachi, T. Ikegami, T. Suzuyama, H. Inaba, S. Okubo, M. Yasuda, F. L. Hong, A. Onae, and K. Hosaka, "Improved frequency measurement of the 1S_0 - 3P_0 clock transition in ^{87}Sr using a Cs fountain clock as a transfer oscillator," *J. Phys. Soc. Jpn.* **84**, 115002 (2015).
52. Y.-G. Lin, Q. Wang, Y. Li, F. Meng, B.-K. Lin, E.-J. Zang, Z. Sun, F. Fang, T.-C. Li, and Z.-J. Fang, "First evaluation and frequency measurement of the strontium optical lattice clock at NIM," *Chin. Phys. Lett.* **32**, 090601 (2015).
53. H. Hachisu, G. Petit, F. Nakagawa, Y. Hanado, and T. Ido, "SI-traceable measurement of an optical frequency at the low 10^{-16} level without a local primary standard," *Opt. Express* **25**, 8511–8523 (2017).
54. H. Hachisu, G. Petit, and T. Ido, "Absolute frequency measurement with uncertainty below 1×10^{-15} using International Atomic Time," *Appl. Phys. B* **123**, 34 (2017).
55. D. Akamatsu, M. Yasuda, H. Inaba, K. Hosaka, T. Tanabe, A. Onae, and F.-L. Hong, "Frequency ratio measurement of ^{171}Yb and ^{87}Sr optical lattice clocks," *Opt. Express* **22**, 7898–7905 (2014).
56. M. Takamoto, I. Ushijima, M. Das, N. Nemitz, T. Ohkubo, K. Yamanaka, N. Ohmae, T. Takano, T. Akatsuka, A. Yamaguchi, and H. Katori, "Frequency ratios of Sr, Yb, and Hg based optical lattice clocks and their applications," *C. R. Physique* **16**, 489–498 (2015).
57. N. Nemitz, T. Ohkubo, M. Takamoto, I. Ushijima, M. Das, N. Ohmae, and H. Katori, "Frequency ratio of Yb and Sr clocks with 5×10^{-17} uncertainty at 150 seconds averaging time," *Nat. Photonics* **10**, 258–261 (2016).
58. J. Grotti, S. Koller, S. Vogt, S. Häfner, U. Sterr, C. Lisdat, H. Denker, C. Voigt, L. Timmen, A. Rolland, F. N. Baynes, H. S. Margolis, M. Zampaolo, P. Thoumany, M. Pizzocaro, B. Rauf, F. Bregolin, A. Tampellini, P. Barbieri, M. Zucco, G. A. Costanzo, C. Clivati, F. Levi, and D. Calonico, "Geodesy and metrology with a transportable optical clock," *Nat. Phys.* **14**, 437–441 (2018).
59. D. Akamatsu, T. Kobayashi, Y. Hisai, T. Tanabe, K. Hosaka, M. Yasuda, and F.-L. Hong, "Dual-mode operation of an optical lattice clock using strontium and ytterbium atoms," *IEEE Trans. Ultrason. Ferroelectr. Freq. Control* **65**, 1069–1075 (2018).
60. M. Fujieda, S. Yang, T. Gotoh, S. Hwang, H. Hachisu, H. Kim, Y. Lee, R. Tabuchi, T. Ido, W. Lee, M. Heo, C. Y. Park, D. Yu, and G. Petit, "Advanced satellite-based frequency transfer at the 10^{-16} level," *IEEE Trans. Ultrason. Ferroelectr. Freq. Control* **65**, 973–978 (2018).
61. M. S. Safronova, D. Budker, D. DeMille, D. F. J. Kimball, A. Derevianko, and C. W. Clark, "Search for new physics with atoms and molecules," *Rev. Mod. Phys.* **90**, 025008 (2017).
62. V. V. Flambaum and A. F. Tedesco, "Dependence of nuclear magnetic moments on quark masses and limits on temporal variation of fundamental constants from atomic clock experiments," *Phys. Rev. C* **73**, 055501 (2006).
63. V. V. Flambaum and V. A. Dzuba, "Search for variation of the fundamental constants in atomic, molecular, and nuclear spectra," *Can. J. Phys.* **87**, 25–33 (2009).
64. T. H. Dinh, A. Dunning, V. A. Dzuba, and V. V. Flambaum, "Sensitivity of hyperfine structure to nuclear radius and quark mass variation," *Phys. Rev. A* **79**, 054102 (2009).
65. V. A. Dzuba and V. V. Flambaum, "Limits on gravitational Einstein equivalence principle violation from monitoring atomic clock frequencies during a year," *Phys. Rev. D* **95**, 015019 (2017).
66. N. Ashby, T. E. Parker, and B. R. Patla, "A null test of general relativity based on a long-term comparison of atomic transition frequencies," *Nat. Phys.* **14**, 822–826 (2018).
67. T. Rosenband, D. B. Hume, P. O. Schmidt, C. W. Chou, A. Brusch, L. Lorini, W. H. Oskay, R. E. Drullinger, T. M. Fortier, J. E. Stalnaker, S. A. Diddams, W. C. Swann, N. R. Newbury, W. M. Itano, D. J. Wineland, and J. C. Bergquist, "Frequency ratio of Al^+ and Hg^+ single-ion optical clocks; metrology at the 17th decimal place," *Science* **319**, 1808–1812 (2008).
68. S. Peil, S. Crane, J. L. Hanssen, T. B. Swanson, and C. R. Ekstrom, "Tests of local position invariance using continuously running atomic clocks," *Phys. Rev. A* **87**, 010102 (2013).